Engineering Analysis with Boundary Elements 34 (2010) 359–368

Contents lists available at ScienceDirect

Engineering Analysis with Boundary Elements

journal homepage: www.elsevier.com/locate/enganabound

Dual reciprocity hybrid boundary node method for acoustic eigenvalue problems

K. Li [a], Q.B. Huang [a,*], Y. Miao [b]

[a] The State Key Laboratory of Digital Manufacturing Equipment and Technology, Huazhong University of Science and Technology, Wuhan, Hubei 430074, PR China
[b] School of Civil Engineering and Mechanics, Huazhong University of Science and Technology, Wuhan, Hubei 430074, PR China

ARTICLE INFO

Article history:
Received 1 July 2009
Accepted 18 October 2009

Keywords:
Hybrid boundary node method
Dual reciprocity method
Moving least squares
Radial basis function
Acoustic eigenvalue problems

ABSTRACT

The hybrid boundary node method (HBNM) is a truly meshless method, and elements are not required for either interpolation or integration. The method, however, can only be used for solving homogeneous problems. For the inhomogeneous problem, the domain integration is inevitable. This paper applied the dual reciprocity hybrid boundary node method (DRHBNM), which is composed by the HBNM and the dual reciprocity method (DRM) for solving acoustic eigenvalue problems. In this method, the solution is composed of two parts, i.e. the complementary solution and the particular solution. The complementary solution is solved by HBNM and the particular one is obtained by DRM. The modified variational formulation is applied to form the discrete equations of HBNM. The moving least squares (MLS) is employed to approximate the boundary variables, while the domain variables are interpolated by the fundamental solutions. The domain integration is interpolated by radial basis function (RBF). The Q–R algorithm and Householder algorithm are applied for solving the eigenvalues of the transformed matrix. The parameters that influence the performance of DRHBNM are studied through numerical examples. Numerical results show that high convergence rates and high accuracy are achievable.

1. Introduction

The acoustic characterization of arbitrarily shaped cavities represents a crucial aspect in several design applications. For transportation vehicles (e.g., aircraft, cars, trains), its importance is not only related to passenger comfort in cabin, but also to the dynamic response of elastic structures interacting with the pressure field arising around them. In the automobile industry, for instance, acoustic eigenvalue analysis is almost routinely performed to design passenger cabins to have acoustic frequencies away from the frequencies of the vibrating engine parts.

Acoustic modes of cavities with complex geometry can only be achieved by using numerical methods, since an exact solution is usually not available. Although Harris and Feshbach [1] applied the perturbation method to dealing with such a problem, the domain and boundary in their paper were very simple. Besides the traditional methods, the finite difference method (FDM) [2], finite element method (FEM) [3] and boundary element method (BEM) [4] have also been widely used to solve these problems.

The advantage in dimensional reducibility makes BEM an attractive numerical analysis tool. Several approaches based on BEM such as complex-valued BEM [5] and the real-part dual BEM [6] have been developed to solve the interior and exterior acoustic problems. Based on the complex-valued BEM, the eigenvalues and eigenmodes can be determined, but complex computation is time consuming. In order to avoid complex computation, Yeih et al. [7] proposed a multiple reciprocity method (MRM) in conjunct with complex-valued BEM and Chen [8] attempted to employ only real-part kernels to solve the eigenproblems.

All of the FDM, FEM and BEM need mesh generation in the preparation of data, and BEM has to face the singular and hypersingular integrals. In order to overcome these difficulties, many researches have paid attention to the meshless method for solving partial differential equation which no longer requires element. In the last decades, many meshless methods have been successfully applied to the eigenproblems of acoustical cavity: Karageorghis [9] employed the method of fundamental solution to calculate the eigenvalues of 2-D cavities. Chen et al. [10] applied the boundary collocation method with radial basis function for acoustic eigenanalysis of 3-D cavities. Christina and Otto [11] employed the radial point interpolation method to analyze the acoustic dispersion characteristics in a 2-D case.

Meshless methods can be divided into two categories. The first one is the domain-type, such as the diffuse element method (DEM) [12], the element free Galerkin (EFG) method [13], the reproducing kernel particle method (RKPM) [14], the point interpolation method (PIM) [15], the meshless local Petrov-galerkin (MLPG) method [16], the local point interpolation

* Corresponding author. Tel.: +862787543971; fax: +862787557664.
E-mail address: qbhuang@mail.hust.edu.cn (Q.B. Huang).

0955-7997/$ - see front matter © 2009 Elsevier Ltd. All rights reserved.
doi:10.1016/j.enganabound.2009.10.012

method (LPIM) [17], etc., and the second is the boundary-type, such as the boundary point interpolation method (BPIM) [18], the boundary node method (BNM) [19], the boundary knot method (BKM) [20,21] hybrid boundary node method (HBNM) [22], etc.

HBNM as a boundary-type meshless method was first proposed by Zhang and Yao [22–25], which uses MLS to approximate the boundary variables, and the integration is limited to a fixed local region. Elements required neither interpolation nor integration. However, it has a drawback of serious 'boundary layer effect', i.e., the accuracy of the result near the boundary is very sensitive to the proximity of the interior points nearby the boundary. To avoid the shortcoming, Miao et al. [26–30] proposed the rigid body-moving method to deal with the singular integration and applied an adaptive integration scheme for solving the boundary layer effect.

Since the governing equation of the acoustic eigenvalue problem has an inhomogeneous term, HBNM cannot solve them without domain integral, which makes the method lose its 'boundary-only' and true meshless character. In this paper, the DRM is introduced to deal with the integral for the inhomogeneous term. DRM was introduced by Nardini and Brebbia [31] for elasto-dynamic problems in 1982 and extended by Wrobel and Brebbia [32] to time dependent diffusion in 1986. The method is essentially a generalized way of constructing particular solution that can be used to solve the inhomogeneous problems as well as to represent any internal source distribution. The method can be applied to defining sources over the whole domain or only on part of it. The aim of DRM is to avoid the domain integral that comes out from the inhomogeneous term of the equations. DRM takes advantage of this fact and builds an approximated particular solution in terms of a linear combination of the RBF.

The dual reciprocity hybrid boundary node method (DRHBNM) is developed by the combination of HBNM and DRM, and DRHBNM has been successfully applied to the elasticity problems [28], transient eddy current problems [33], free vibration problems [34], etc. However, applications concerning acoustic problem and in particular an investigation of the acoustic eigenvalue problem has not been conducted yet. In this paper, DRHBNM is applied for solving acoustic eigenvalue problem. The solution of the governing equation is composed of two parts: complementary solution and particular solution. For the first part, the same as HBNM, the variables inside the domain are interpolated by the fundamental solution, while the unknown boundary variables are approximated by the MLS approximation. The modified variational formulation is applied to forming the discretized equations of HBNM. For the second part, DRM has been used and the RBF are applied to interpolating the inhomogeneous part of the equations. Because of the inhomogeneous term of the governing equations, the boundary integral equations obtained by DRHBNM are not enough to solve all variables. Some additional equations are proposed to obtain the relation of the variables in the domain and on the boundary.

DRHBNM is a truly meshless method, and elements are not required for either interpolation or integration, only discrete nodes are constructed on the boundary of a domain, several nodes in the domain are needed just for the RBF interpolation. The rigid body-moving method has been applied to overcoming the singular integration. An adaptive integration scheme has been employed to solve the boundary layer effect. The numerical examples show that the accuracy and convergence of DRHBNM are high, and the pre-processing is very easy, although much less amount of nodes are used, excellent results can be obtained. The parameters that influence the performance and efficiency of the method are also studied through numerical examples.

This paper is organized as follows: the detailed description of the acoustic eigenvalue problem is shown in Section 2; a review of the HBNM will be discussed in Section 3; the DRHBNM for acoustic eigenvalue problem is formulated in Section 4; numerical implementation is demonstrated in Section 5; numerical examples for 2D and 3D acoustic eigenproblems are shown in Section 6; finally, the paper will end with conclusions in Section 7.

2. Acoustic eigenvalue problem

The propagation of pressure waves in an acoustic fluid inside a domain Ω is governed by the wave equation, which can be derived using the balance of mass and momentum as well as the ideal gas law. Provided that the state variables pressure P, density ρ, and velocity v experience only small variations, the wave equation

$$\nabla^2 P - \frac{1}{c^2}\frac{\partial^2 P}{\partial t^2} = 0 \tag{1}$$

is obtained, where ∇^2 is the Laplace operator, c denotes the sound velocity. For time harmonic waves of frequency ω, the pressure can be written as

$$P(x,t) = \mathrm{Re}(p(x)e^{-i\omega t}) \tag{2}$$

where p is the complex amplitude of the sound pressure. Introducing the wave number $k=\omega/c$, leads to the objective equation

$$\nabla^2 p + k^2 p = 0 \tag{3}$$

The boundary Γ of the fluid domain Ω is decomposed into three distinct regions Γ_D, Γ_N and Γ_R such that

$$\boldsymbol{\Gamma} = \boldsymbol{\Gamma}_D \cup \boldsymbol{\Gamma}_N \cup \boldsymbol{\Gamma}_R \tag{4}$$

The associated boundary conditions are

Dirichlet boundary conditions on Γ_D:

$$p = \overline{p} \tag{5}$$

Neumann boundary conditions on Γ_N:

$$\frac{\partial p}{\partial n} = -i\omega\rho\overline{v}_n \tag{6}$$

Mixed (Robin) boundary conditions on Γ_R:

$$\frac{\partial p}{\partial n} = -i\rho A_n p \tag{7}$$

where A_n represents the admittance, n is the normal vector, and v_n the normal velocity.

In the conventional BEM, the fundamental solution of Helmholtz differential operator is applied, which is defined by

$$-(\nabla^2 + k^2)G_k(x,s) = \delta(x,s) \tag{8}$$

where x are the coordinates of field points and s are the coordinates of source points. Then, the fundamental solutions are obtained:

$$G_k(x,s) = \begin{cases} \dfrac{-i}{4}H_0^{(2)}(k|x-s|) & 2\text{-}D \\ \dfrac{1}{4\pi|x-s|}e^{-ik|x-s|} & 3\text{-}D \end{cases} \tag{9}$$

where $H_0^{(2)}(k|x-s|)$ is the second Hankel function of zeroth order. In the fundamental solutions $G_k(x,s)$, whether the Hankel function or the exponential function, is a transcendental function of frequency [4], thus, serious difficulty may be encountered in the numerical calculation. For instance, in the evaluation of eigenvalues, the eigenequation is transcendental. An alternative approach is employing the fundamental solutions of the Laplace differential operator which are independent of the frequency k, and the inhomogeneous term can be solved by DRM.

3. Review of the HBNM

Consider the wave equation (3), can be rewritten as

$$\nabla^2 p = -k^2 p \tag{10}$$

As a consequence, the left-hand side of Eq. (10) can be dealt with by HBNM for the Laplace equation, and the integrals corresponding to the right-hand side are taken into the boundary using RBF interpolation. In DRHBNM, the solution variables p can be divided into complementary solutions p^c and particular solutions p^k, i.e.

$$p = p^c + p^k \tag{11}$$

The particular solution p^k just needs to satisfy the inhomogeneous equation in total space as follows:

$$\nabla^2 p^k = -k^2 p \tag{12}$$

The complementary solution p^c must satisfy the Laplace equation and the modified boundary condition, they can be written as

$$\nabla^2 p^c = 0 \tag{13}$$

$$p^c = \overline{p}^c = \overline{p} - p^k \tag{14}$$

$$v^c = \overline{v}^c = \overline{v} - v^k \tag{15}$$

in which $\overline{p}$, $\overline{v}$ are the boundary node values of each node on the boundary, and $\overline{p}^c$, $\overline{v}^c$ are the generous solution of boundary nodes.

In the following, the complementary solution will be solved by the HBNM.

The HBNM is based on a modified variational principle. The functions in the modified principle assumed to be independent are: pressure field within the domain p, boundary pressure field $\tilde{p}$, and boundary normal velocity $\tilde{v}$. Consider a domain Ω enclosed by $\Gamma = \Gamma_D + \Gamma_N$ with prescribed pressure $\overline{p}$ and normal velocity $\overline{v}$ at the boundary portions Γ_D and Γ_N, respectively. The corresponding variational function Π_{AB} is defined as

$$\prod_{AB} = \int_\Omega \frac{1}{2} p_{,i} p_{,i}\, d\Omega - \int_\Gamma \tilde{v}(p-\tilde{p}) d\Gamma - \int_{\Gamma_N} \overline{v}\tilde{p}\, d\Gamma \tag{16}$$

where $\tilde{v}$ and $\tilde{p}$ are the boundary node values which are approximated by MLS, p is the internal node value, and the boundary pressure $\tilde{p}$ satisfies the Dirichlet boundary condition, i.e. $\overline{p} = \tilde{p}$, on Γ_D.

With the vanishing of $\delta\Pi_{AB}$ over the domain and its boundary, the following equivalent integral can be obtained:

$$\int_\Gamma (v-\tilde{v})\delta\tilde{p}\, d\Gamma - \int_\Omega p_{,ii}\delta\tilde{p}\, d\Omega = 0 \tag{17}$$

$$\int_\Gamma (p-\tilde{p})\delta\tilde{v}\, d\Gamma = 0 \tag{18}$$

$$\int_{\Gamma_N} (\tilde{v}-\overline{v})\delta p\, d\Gamma = 0 \tag{19}$$

Eq. (19) will be satisfied if the Neumann boundary condition, $\tilde{v} = \overline{v}$, is imposed. So, it will be ignored in the following.

Because the variational principle is an universal theory, Eqs. (17) and (18) should be satisfied in any sub-domain Ω_S, which is bounded by Γ_S and L_S (see Fig. 1). The weak forms on a sub-domain Ω_S and its boundary, Γ_S and L_S are used to replace Eqs. (17) and (18). At the same time, test function $h_J(Q)$ is used to replace the variational part. They can be presented as

$$\int_{\Gamma_S + L_S} (v-\tilde{v}_s) h\, d\Gamma - \int_{\Omega_S} p_{,ii} h\, d\Omega = 0 \tag{20}$$

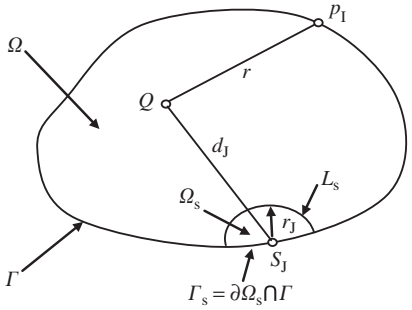

Fig. 1. Local domain and source point of fundamental solution corresponding to S_J.

$$\int_{\Gamma_S + L_S} (p-\tilde{p}_s) h\, d\Gamma = 0 \tag{21}$$

The shape and dimension of the sub-domains may be arbitrary. Obviously, a circle is the simplest regularly shaped sub-domain in the two-dimensional space. The sub-domain Ω_S is chosen as the intersection of domain Ω and a circle centered at a boundary node S_J, and the radius of the circle is r_J (Fig. 1).

We approximate $\tilde{p}_s$ and $\tilde{v}_s$ at the boundary Γ by the MLS approximation as

$$\tilde{p}(s) = \sum_{I=1}^{N} \boldsymbol{\Phi}_I(s)\hat{p}_I \tag{22}$$

$$\tilde{v}(s) = \sum_{I=1}^{N} \boldsymbol{\Phi}_I(s)\hat{v}_I \tag{23}$$

where N stands for the number of nodes located on the surface, $\hat{p}_I$ and $\hat{v}_I$ are the nodal values, and $\Phi_I(s)$ is the shape function of the MLS approximation, corresponding to node S_I, which is given by

$$\boldsymbol{\Phi}_I(s) = \sum_{j=1}^{m} \psi_j(s)[\mathbf{A}^{-1}(s)\mathbf{B}(s)]_{jI} \tag{24}$$

Matrices $\mathbf{A}(s)$ and $\mathbf{B}(s)$ are defined as

$$\mathbf{A}(s) = \sum_{I=1}^{N} \omega_i(s)\psi(s_I)\psi^T(s_I) \tag{25}$$

$$\mathbf{B}(s) = [\omega_1(s)\psi(s_1), \omega_2(s)\psi(s_2), \ldots, \omega_N(s)\psi(s_N)] \tag{26}$$

where $\omega(s)$ is the weight matrix for the boundary variables. This is a diagonal matrix with the diagonal elements $\omega_I(s)$. $\psi(s)$ is a vector of the basis function of the order m. In this study, we take $m=3$, namely, $\psi^T(s)=[1,s,s^2]$, where s is a parameter coordinate and denotes the distance between the point in the domain and the source point on the boundary.

The weight functions play an important role in the meshless methods. Most meshless weight functions are bell-shaped. In the present study, Gaussian weight function is chosen and can be written as

$$\omega_I(s) = \begin{cases} \dfrac{\exp[-(d_I/c_I)^2] - \exp[-(\hat{d}_I/c_I)^2]}{1-\exp[-(\hat{d}_I/c_I)^2]} & 0 \le d_J \le \hat{d}_I \\ 0 & d_J \ge \hat{d}_I \end{cases} \tag{27}$$

where $d_I = |s - s_I|$ is the distance between an evaluation point and node s_I, c_I is a constant controlling the shape of the weight function $\omega_I(s)$ and, therefore, is the relative weights, and $\hat{d}_I$ is the size of the support domain for the weight function $\omega_I(s)$ and it determines the support of node s_I.

In Eqs. (20) and (21), $\tilde{p}_s$ and $\tilde{v}_s$ at Γ_S can be represented by $\tilde{p}$ and $\tilde{v}$ expressed in Eqs. (22) and (23) since Γ_S is a portion of Γ, while $\tilde{p}_s$ and $\tilde{v}_s$ at L_S have not been defined yet. To solve this problem, we select h such that all integrals vanish over L_S. This can

be easily accomplished by using the weight function in the MLS approximation for h, with the half-length of the major axis d_I of the support of the weight function being replaced by the radius of the sub-domain Ω_S, i.e.

$$h_J(Q)=\begin{cases}\dfrac{\exp[-(d_J/c_J)^2]-\exp[-(r_J/c_J)^2]}{1-\exp[-(r_J/c_J)^2]} & 0\le d_J\le r_J\\ 0 & d_J\ge r_J\end{cases} \tag{28}$$

where d_J is the distance between point Q in the domain and the nodal point s_J. On L_S, $d_J=r_J$, from Eq. (28) it can be seen that $h_J(Q)=0$, so it vanishes on boundary L_S. Eqs. (20) and (21) can be rewritten as

$$\int_{\Gamma_s}(v-\tilde{v}_s)h\,d\Gamma-\int_{\Omega_s}p_{,ii}h\,d\Omega=0 \tag{29}$$

$$\int_{\Gamma_s}(p-\tilde{p}_s)h\,d\Gamma=0 \tag{30}$$

The domain variables p is interpolated by the fundamental solution

$$p=\sum_{I=1}^{N}p_I^s x_I \tag{31}$$

And hence at the boundary node, the normal velocity is given by

$$v=\sum_{I=1}^{N}\frac{\partial p_I^s}{\partial n}x_I \tag{32}$$

where p_I^s is the fundamental solution, x_I are unknown parameters, N is the total number of boundary nodes, n is the outward normal vector to the boundary Γ. The fundamental solution is written as

$$p_I^s=\frac{\ln r(Q,s_I)}{2\pi} \tag{33}$$

where Q and s_I are field point and source point, respectively, r is the distance between source point s_I and field point Q.

As p is expressed by Eq. (31), the second term on the left-hand side of Eq. (29) vanishes if one does not include node s_I, at which the singularity occurs, from the sub-domain Ω_S. This singularity will be taken into account when the boundary integrals are evaluated. By substituting Eqs. (22), (23), (28), (31) and (32) into Eqs. (29) and (30), and omitting the vanishing terms, we have

$$\sum_{I=1}^{N}\int_{\Gamma_s}\frac{\partial p_I^s}{\partial n}h_J(Q)x_I\,d\Gamma=\sum_{I=1}^{N}\int_{\Gamma_s}\Phi_I(s)h_J(Q)\hat{v}_I\,d\Gamma \tag{34}$$

$$\sum_{I=1}^{N}\int_{\Gamma_s}p_I^s h_J(Q)x_I\,d\Gamma=\sum_{I=1}^{N}\int_{\Gamma_s}\Phi_I(s)h_J(Q)\hat{p}_I\,d\Gamma \tag{35}$$

Using the above equations for all nodes, one can get the system equations

$$\mathbf{Tx}=\mathbf{H}\hat{\mathbf{v}}^c \tag{36}$$

$$\mathbf{Ux}=\mathbf{H}\hat{\mathbf{p}}^c \tag{37}$$

where

$$T_{IJ}=\int_{\Gamma_s}\frac{\partial p_I^s}{\partial n}h_J(Q)d\Gamma \tag{38}$$

$$H_{IJ}=\int_{\Gamma_s}\Phi_I(s)h_J(Q)d\Gamma \tag{39}$$

$$U_{IJ}=\int_{\Gamma_s}p_I^s h_J(Q)d\Gamma \tag{40}$$

Matrices **U** and **T** in the present method are much simpler than those obtained in BEM and BNM. Because the variables interpolation is on the independent boundary segment, matrix **H** is also sparse.

4. The DRHBNM

Based on the HBNM, the DRHBNM will be developed in this section, which is combination of the HBNM with the DRM. The complementary solution has been solved successfully by HBNM, and then the DRM will be applied for solving the particular solution.

4.1. DRM

The DRM can be used in acoustic eigenvalue problems to transform the domain integral arising from the application of inhomogeneous to equivalent boundary integral. Applying interpolation for inhomogeneous term, the following approximation can be proposed for the term $-k^2p$:

$$-k^2p=\sum_{j=1}^{N+L}f^j\alpha^j \tag{41}$$

where the α^j are a set of initially unknown coefficients, the f^j are approximation functions. N and L are the total number of boundary nodes and total number of interior nodes, respectively.

Same as Eq. (41), the particular solution can be interpolated by the basis form of the particular solution. It can be written as follows:

$$p_I^k\approx\sum_{j=1}^{N+L}\bar{\bar{p}}_I^j\alpha^j \tag{42}$$

where $\bar{\bar{p}}_I^j$ is the basis form of particular solution.

If p^k satisfies Eq. (12), the following equations can be obtained:

$$\nabla^2\bar{\bar{p}}^j=f^j \tag{43}$$

The approximation function, f^j, can be chosen as $f^j=1+r+r^2$. Obviously, the particular solution $\bar{\bar{p}}$ satisfying Eq. (43) can be obtained as

$$\bar{\bar{p}}=\frac{r^2}{4}+\frac{r^3}{9}+\frac{r^4}{16} \tag{44}$$

The corresponding expression for the normal velocity $\bar{\bar{v}}$ is

$$\bar{\bar{v}}=\left(r_{,x}\frac{\partial x}{\partial n}+r_{,y}\frac{\partial y}{\partial n}\right)\left(\frac{1}{2}+\frac{r}{3}+\frac{r^2}{4}\right) \tag{45}$$

Solving Eqs. (41)–(43), the particular solution can be written in matrix form as follows:

$$\mathbf{p}^k=-k^2\bar{\bar{\mathbf{p}}}\mathbf{F}^{-1}\mathbf{p} \tag{46}$$

$$\mathbf{v}^k=-k^2\bar{\bar{\mathbf{v}}}\mathbf{F}^{-1}\mathbf{p} \tag{47}$$

where each column of **F** consists of a vector f^j containing the values of the function f^j at the DRM collocation nodes. $\bar{\bar{\mathbf{p}}}$ and $\bar{\bar{\mathbf{v}}}$ are the matrix forms of the basis type of particular solutions.

4.2. DRHBNM

For a well-posed problem, either $\tilde{p}$ or $\tilde{v}$ is known at each node on the boundary. However, transformation between $\hat{p}_I$ and $\tilde{p}_I$. $\hat{v}_I$ and $\tilde{v}_I$ is necessary because the MLS approximation lacks the delta function property. For the panels where $\tilde{p}_I$ is prescribed, $\tilde{p}_I$ is

related to $\hat{p}_I$ by [35]

$$\hat{p}_I = \sum_{J=1}^{N_t} R_{IJ}\tilde{p}_J = \sum_{J=1}^{N_t} R_{IJ}\overline{p}_J \tag{48}$$

and for the panels where $\tilde{v}_I$ is prescribed, $\tilde{v}_I$ is related to $\hat{v}_I$ by

$$\hat{v}_I = \sum_{J=1}^{N_t} R_{IJ}\tilde{v}_J = \sum_{J=1}^{N_t} R_{IJ}\overline{v}_J \tag{49}$$

where $R_{IJ} = [\boldsymbol{\Phi}_J(s_I)]^{-1}$, N_t is the total number on a piece of the edge and $\overline{p}_J$ and $\overline{v}_J$ are the related nodal values.

Substituting Eqs. (46)–(49) into Eq. (11), then substituting the result into Eqs. (36) and (37), we can obtain

$$\mathbf{Ux} = \mathbf{HR}(\mathbf{p}-\mathbf{p}^k) = \mathbf{HR}(\mathbf{p}+k^2\overline{\overline{\mathbf{p}}}\mathbf{F}^{-1}\mathbf{p}) \tag{50}$$

$$\mathbf{Tx} = \mathbf{HR}(\mathbf{v}-\mathbf{v}^k) = \mathbf{HR}(\mathbf{v}+k^2\overline{\overline{\mathbf{v}}}\mathbf{F}^{-1}\mathbf{p}) \tag{51}$$

Eqs. (50) and (51) are the system equations of the DRHBNM for acoustic eigenvalue problems. Assuming that N nodes are located on the boundary, we can get N unknown variables on the boundary from Eqs. (50) and (51). However, the equations above include the pressure of the L internal nodes, and so the additional equations are needed.

4.3. Additional equations

Eqs. (50) and (51) cannot be solved for the variables of the internal nodes and additional equations for Helmholtz problem will be developed in this section.

The unknown variables of the internal nodes can be expressed as follows:

$$p^* = p^c + p^k \tag{52}$$

The complementary solution p^c can be interpolated by the fundamental solution and the particular solution p^k can be expressed by Eq. (46). So, Eq. (52) can be rewritten as

$$\mathbf{p}^* = \mathbf{p}^s\mathbf{x} - k^2\overline{\overline{\mathbf{p}}}\mathbf{F}^{-1}\mathbf{p} \tag{53}$$

where $\mathbf{p}^*$ is the pressure of the internal nodes, $\mathbf{p}^s$ is the matrix of the fundamental solution on each internal node and $\overline{\overline{\mathbf{p}}}$ is the matrix of values of basis type of particular solution.

Solving out the coefficient vector $\mathbf{x}$ in Eq. (50), we can obtain

$$\mathbf{x} = \mathbf{U}^{-1}\mathbf{HR}(\mathbf{p}+k^2\overline{\overline{\mathbf{p}}}\mathbf{F}^{-1}\mathbf{p}) \tag{54}$$

Substituting Eq. (54) into Eq. (53), we get

$$\mathbf{p}^* = \mathbf{p}^s\mathbf{U}^{-1}\mathbf{HRp} + k^2\mathbf{p}^s\mathbf{U}^{-1}\mathbf{HR}\overline{\overline{\mathbf{p}}}\mathbf{F}^{-1}\mathbf{p} - k^2\overline{\overline{\mathbf{p}}}\mathbf{F}^{-1}\mathbf{p} \tag{55}$$

Substituting Eq. (54) into Eq. (51), we get

$$\mathbf{TU}^{-1}\mathbf{HR}(\mathbf{p}+k^2\overline{\overline{\mathbf{p}}}\mathbf{F}^{-1}\mathbf{p}) = \mathbf{HR}(\mathbf{v}+k^2\overline{\overline{\mathbf{v}}}\mathbf{F}^{-1}\mathbf{p}) \tag{56}$$

Combining Eq. (55) with Eq. (56), one can obtain

$$\mathbf{p}\hat{\mathbf{H}} - v\hat{\mathbf{G}} = -k^2\mathbf{Sp} \tag{57}$$

where

$$\hat{\mathbf{H}} = \begin{bmatrix} \mathbf{TU}^{-1}\mathbf{HR} & \mathbf{0} \\ \mathbf{p}^S\mathbf{U}^{-1}\mathbf{HR} & -\mathbf{I} \end{bmatrix} \tag{58}$$

$$\hat{\mathbf{G}} = \begin{bmatrix} \mathbf{HR} \\ \mathbf{0} \end{bmatrix} \tag{59}$$

$$\mathbf{S} = \begin{bmatrix} \mathbf{TU}^{-1}\mathbf{HR}\overline{\overline{\mathbf{p}}}\mathbf{F}^{-1} - \mathbf{HR}\overline{\overline{\mathbf{v}}}\mathbf{F}^{-1} \\ \mathbf{p}^S\mathbf{U}^{-1}\mathbf{HR}\overline{\overline{\mathbf{p}}}\mathbf{F}^{-1} - \overline{\overline{\mathbf{p}}}\mathbf{F}^{-1} \end{bmatrix} \tag{60}$$

Take an acoustic eigenvalue problem, an enclosing cavity, as an example. The external pressure is set to zero, and the boundary condition of pressure is also set to zero, i.e.

$$\mathbf{p}_1 = \{0\}, \quad \mathbf{v}_2 = \{0\} \tag{61}$$

Imposed the boundary condition, Eq. (57) can be assembled into the following system of equation:

$$\mathbf{Kp} = k^2\mathbf{Mp} \tag{62}$$

where

$$\mathbf{K} = \hat{\mathbf{H}}_{22} - \hat{\mathbf{G}}_{21}\hat{\mathbf{G}}_{11}^{-1}\hat{\mathbf{H}}_{12} \tag{63}$$

$$\mathbf{M} = -(\mathbf{S}_{22} - \hat{\mathbf{G}}_{21}\hat{\mathbf{G}}_{11}^{-1}\mathbf{S}_{12}) \tag{64}$$

K and **M** represent acoustic stiffness and acoustic mass matrix, respectively. Eq. (62) represents a generalized algebraic eigenvalue problem, the solution of which can be obtained directly by a variant of the subspace iteration scheme.

5. Numerical implementation

5.1. Singular integral

It is obvious that the integrals in Eqs. (38) and (40) consist of regular and singular ones. The regular integrals can be evaluated using the usual Gaussian quadrature based on the regular boundary Γ_S. The singular integrals in Eqs. (38) and (40) are different and they should be treated by different methods.

The main diagonal term of matrix **U** in Eq. (40) involves a logarithm singular integral. This type of singular integral can be calculated by a modified Gauss quadrature as follows:

$$I = \int_0^1 \ln\left(\frac{1}{\xi}\right) f(\xi)\,d\xi = \sum_{i=1}^{n} f(\xi_i)\omega_i \tag{65}$$

where ξ_i and ω_i are the integration points and weight factors, respectively. They are the same as the conventional BEM.

However, the main diagonal terms of matrix **T** in Eq. (38) involves a $(1/r)$ type singular integral and cannot be dealt with by the usual method directly. In order to avoid the calculation of hypersingular integral, the rigid body-moving method is applied as BEM.

For a two-dimensional Helmholtz problem, two groups of particular solutions of rigid body-moving method are applied. They are both constant pressure fields and can be described as follows:

$$p_x = 0, \quad p_y = 1, \quad v_x = v_y = 0 \tag{66}$$

$$p_x = 1, \quad p_y = 0, \quad v_x = v_y = 0 \tag{67}$$

Substituting Eqs. (66) and (67) into Eqs. (36) and (37), one can obtain

$$\mathbf{TU}^{-1}\mathbf{H}\{\mathbf{p}\} = \mathbf{H}\{\mathbf{0}\} \tag{68}$$

where $\{\mathbf{0}\}$ is a column vector with all elements equal to zero. Substituting the two groups of the pressure particular solutions into Eq. (68), respectively, the values of the main diagonal of **T** can be obtained.

5.2. Adaptive integration scheme

Like other boundary-type methods, the present method has a drawback of 'boundary-layer effect'. To avoid this drawback, an adaptive integration scheme was applied.

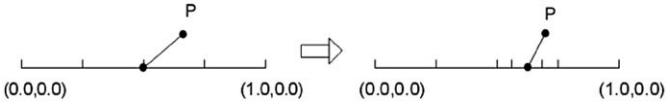

Fig. 2. Subdividing of a segment in the parametric space to the evaluation point P.

Table 1
First four lowest eigenvalues of the rectangular cavity.

Mode no.	Exact solution	Present method	FEM (ANSYS; 3200 elements)	FEM (ANSYS; 7200 elements)
1st	3.72419	3.72449	3.72583	3.72492
2nd	5.08622	5.08698	5.09014	5.08796
3rd	6.59382	6.59553	6.60203	6.59747
4th	6.77271	6.77454	6.78057	6.77620

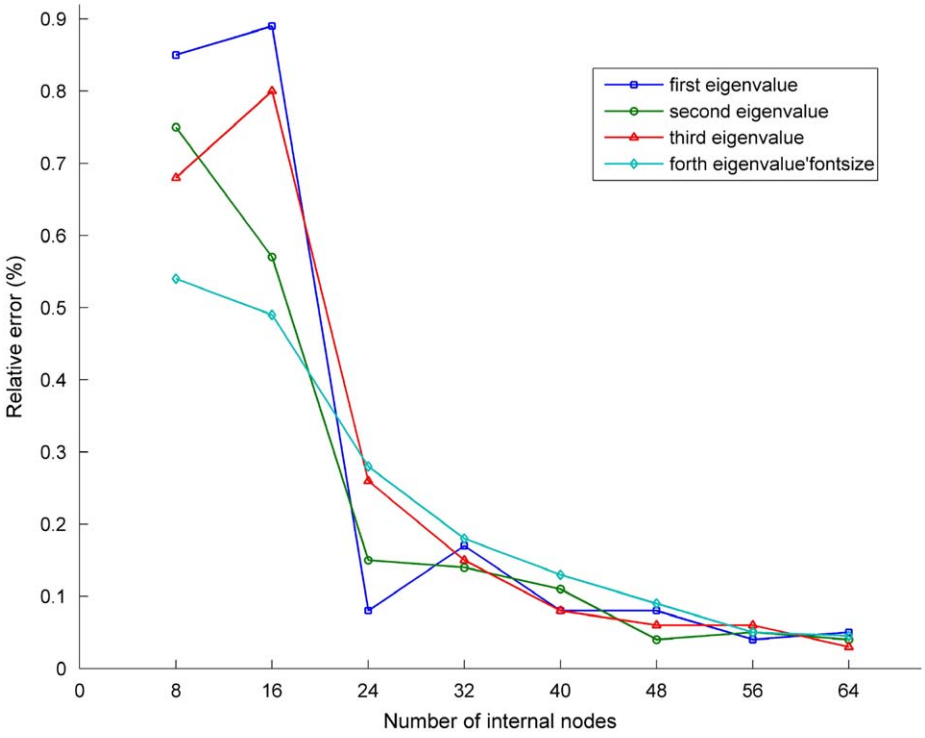

Fig. 3. Relative error of the eigenvalue with different internal nodes.

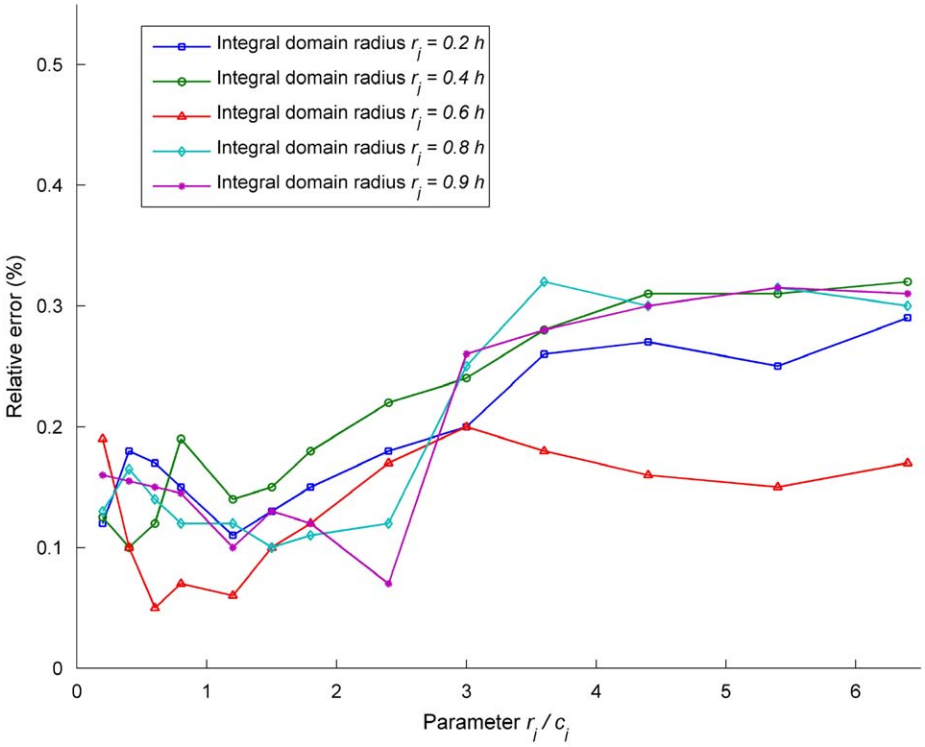

Fig. 4. Relative error of the first eigenvalue with different r_j.

The pressure p at an internal point P, is evaluated by the traditional boundary integral equation as follows:

$$\mathbf{p}(P) = \int_\Gamma \mathbf{p}(Q,P)\tilde{v}(Q)\,d\boldsymbol{\Gamma} - \int_\Gamma \mathbf{v}(Q,P)\tilde{p}(Q)\,d\boldsymbol{\Gamma} = \sum_{N_s}\int_{\boldsymbol{\Gamma}} \mathbf{p}(Q,P)\tilde{v}(Q)\,d\boldsymbol{\Gamma} - \sum_{N_s}\mathbf{v}(Q,P)\tilde{p}(Q)\,d\boldsymbol{\Gamma} \tag{69}$$

where $\mathbf{p}(Q,P)$ is the fundamental solution with Q and P being the field point and source point, respectively. N_s denotes the number of the segments which compose the whole boundary. Every segment is represented by a unit sector in the parametric space. First, the unit sector is divided into four equal quarters (see Fig. 2). For each quarter, the quarter length l, and the distance between the evaluation point and the centre of the quarter, d, in the rectangular coordinate system can be calculated. If l is smaller than d, this quarter is taken as a regular integration segment. It will be divided further into sub-quarters, until all segments become regular. Finally, use Gaussian quadrature for all segments, the integrals in Eq. (69) can be calculated accurately. It should be pointed that the segment shown in Fig. 2 is in the parametric space and is not the boundary element.

5.3. Eigenvalue and eigenvector

It should be pointed out that, in Eq. (62), neither **K** nor **M** is symmetric or positive definite, so that care should be taken in the choice of the appropriate eigenvalue solution algorithm.

The method employed by Nardini and Brebbia [31] reduced the generalized eigenvalue problem to a standard one by the inversion of matrix **K**, and obtained the following system:

$$\mathbf{Ap} = \lambda\mathbf{p} \tag{70}$$

with

$$\mathbf{A} = \mathbf{K}^{-1}\mathbf{M} \tag{71}$$

$$\lambda = 1/k^2 \tag{72}$$

The Q–R algorithm is chosen to solve eigenfrequencies. In order to improve the convergence, matrix A is transformed firstly into tri-diagonal form by the Householder algorithm. Then the eigenvalues and eigenvectors of the transformed matrix are calculated by the Q–R algorithm. For the large systems, a variant of the subspace iteration method is used for the nonsymmetric matrices [27,31].

The Q–R algorithm is described as follows:

Assume $\mathbf{A}_1 = \mathbf{A}$, note $\mathbf{A_r} = [a_{ij}^{(r)}]_{n\times n}$, and set $\mathbf{Q}_1 = \mathbf{I}$, where $\mathbf{I}$ is a unit matrix. For $r = 1,2,3,\ldots,n-1$ calculate according the following programs:

(1) If $a_{ij}^{(r)}(r = r+1, r+2, \ldots, n)$ are equal to zero, assume $\mathbf{Q}_{r+1} = \mathbf{Q}_r$, $\mathbf{A}_{r+1} = \mathbf{A}_r$, and go to (5), otherwise go to (2).

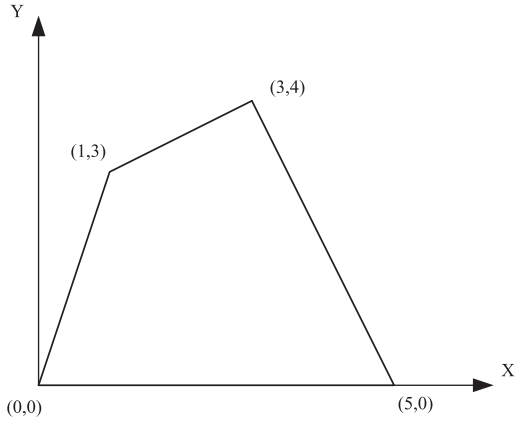

Fig. 6. Quadrilateral cavity.

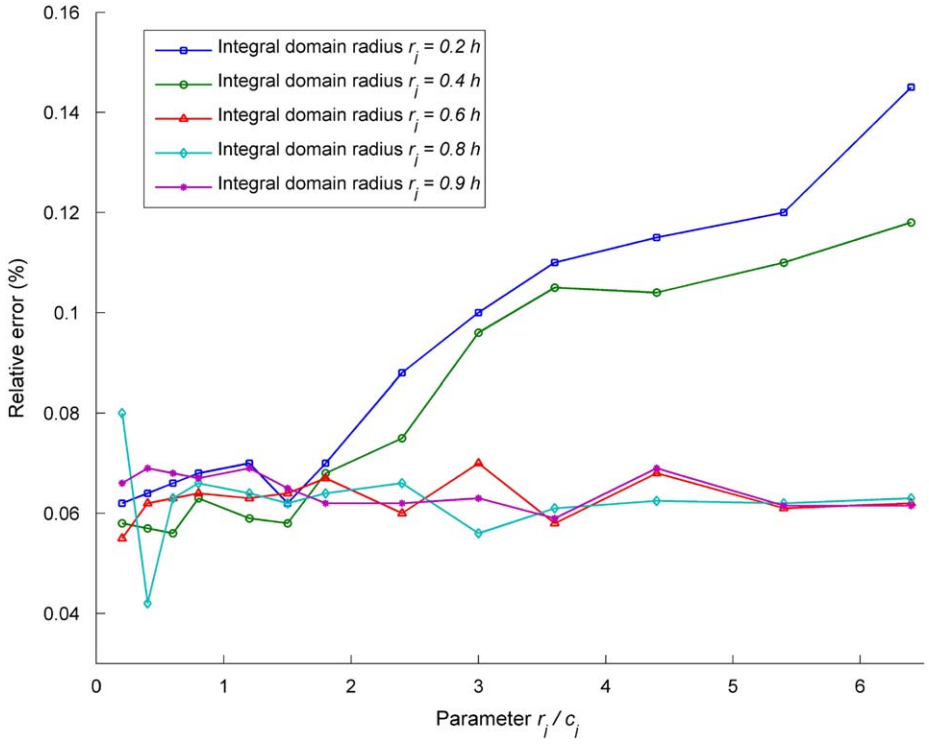

Fig. 5. Relative error of the second eigenvalue with different r_j.

(2) Calculate the following equations:

$$d_r = \sqrt{\sum_{i=r}^{n} (a_{ir}^{(r)})^2}$$

$$c_r = -sign(a_{rr}^{(r)}) d_r$$

If $a_{rr}^{(r)} = 0$, then note $c_r = d_r$

$$h_r = c_r^2 - c_r a_{rr}^{(r)}$$

(3) Assume $\mathbf{p_r} = (0,\ldots,0,a_{rr}^{(r)} - c_r, a_{r+1,r}^{(r)},\ldots,a_{n,r}^{(r)})^T$

Table 2
First five lowest eigenfrequencies of the quadrilateral cavity.

Mode no.	FEM (Hz)	Kim's method (Hz) [36]		Present method (Hz)	
		N_{el}=25	N_{el}=1600	N_i=8	N_i=32
1st	43.179	43.738	43.188	43.350	43.190
2nd	47.291	48.034	47.302	47.506	47.304
3rd	77.304	79.540	77.340	78.269	77.365
4th	80.400	84.479	80.465	81.565	80.474
5th	91.654	97.608	91.0.746	93.293	91.757

(4) Calculate $k_r = \mathbf{Q_r p_r}$

$$\mathbf{Q}_{r+1} = \mathbf{Q_r} - k_r \mathbf{p}_r^T / \mathbf{h_r}$$

$$\mathbf{P_r} = \mathbf{A}_r^T \mathbf{p_r} / \mathbf{h_r}$$

$$\mathbf{A}_{r+1} = \mathbf{A_r} - \mathbf{p_r} \mathbf{P}_r^T$$

(5) If $r = n-1$, stop calculation, otherwise go to (1).

If calculation is over, an upper triangular matrix **A** is obtained, and **A=QR**, the eigenvalues of **A** are the same as the original matrix. Based on the above, an iteration method is obtained as

$$\begin{cases} \mathbf{A_1} = \mathbf{A} \\ \mathbf{A_k} = \mathbf{Q_k R_k} \\ \mathbf{A_k} = \mathbf{A}_{k+1} \mathbf{Q_k} \end{cases} \quad \text{(decomposition by the Q-R algorithm)}$$

If iteration is over, the elements under the diagonal are close to zero, and the diagonal elements are eigenvalues.

6. Numerical examples

A number of examples are presented to illustrate the effectiveness of this method for acoustic eigenvalue problems. The parameters that influence the performance of the method

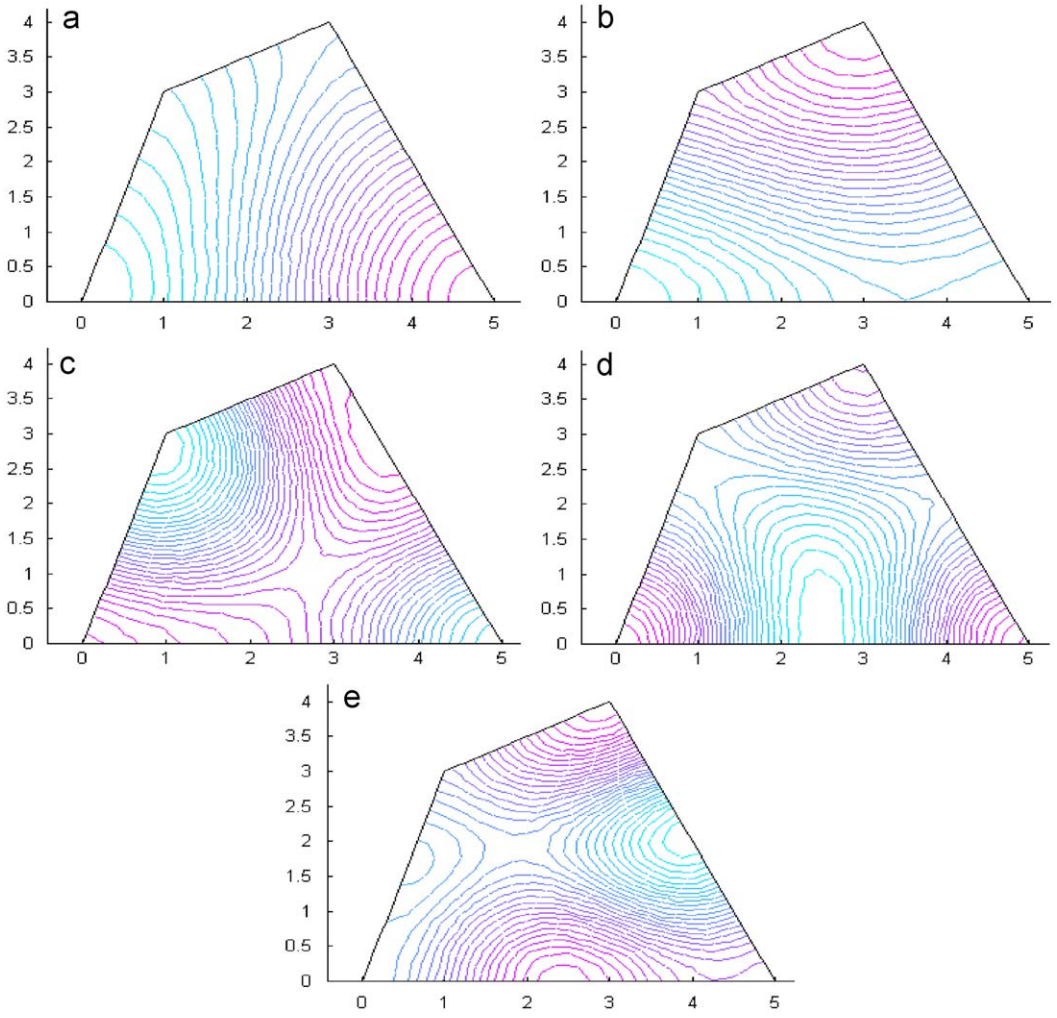

Fig. 7. Contours of the four lowest eigenmode obtained by the present method: (a) the first eigenmode; (b) the second eigenmode; (c) the third eigenmode; (d) the forth eigenmode; (e) the fifth eigenmode.

are also investigated. The high accuracy of the eigenvalues obtained by the present method is demonstrated and compared with those obtained by the FEM or BEM. For the purpose of error estimation and convergence studies, the relative error is defined as

$$e = \frac{|p^{(n)} - p^{(e)}|}{p^{(e)}} \tag{73}$$

where the superscripts (e) and (n) refer to the exact and the numerical solutions, respectively.

In these examples, the support size for the weight function $\hat{d}_I$ is taken to be 3.5 h and the radius of the sub-domain r_J is chosen as 0.9 h, with h being the average distance of the adjacent nodes. The parameter c_I is taken to be $d_I/c_I = 0.5$, and the parameter c_J is taken to be $r_J/c_J = 1.2$. To deal with the normal velocity discontinuities at the corners, the nodes are not arranged at these locations and the support domain for interpolation is truncated.

6.1. Rectangular cavity with Dirichlet boundary condition

In the first example, we consider the following acoustic eigenvalue problem with Dirichlet boundary condition:

$$\begin{cases} \nabla^2 p(\mathbf{x}) + k^2 p(\mathbf{x}) = 0, & \mathbf{x} = \left\{(x,y) | 0 \le x \le \dfrac{\pi}{2} \cap 0 \le y \le 1\right\} \\ p(\mathbf{x}) = 0, & \mathbf{x} = \left\{(x,y) | \left(x = 0, \dfrac{\pi}{2} \cap 0 \le y \le 1\right) \cup \left(y = 0, 1 \cap 0 \le x \le \dfrac{\pi}{2}\right)\right\} \end{cases} \tag{74}$$

The rectangular cavity is discretized using 12 nodes on each long edge and 8 nodes on each short edge. A total of 40 boundary nodes are located on the boundary and 24 internal nodes are arranged in the domain.

The eigenvalues for the first four eigenvalue are given in Table 1. The results are generally accurate up to 10^{-3} compared with the exact solutions, these results are much more accurate than those obtained by the FEM. In FEM analysis by ANSYS, 3200 elements and 7200 elements were used. It can be seen that even though the number of nodes is relatively small, a good result still can be obtained by the present method.

In order to test the sensitivity of the present method to the number of the internal nodes, eight other discretizations with different number of internal nodes were applied. The relative errors for each nodal arrangement in the DRHBNM computations are presented in Fig. 3. It can be seen that the more the points are arranged in the domain, the more the accurate solution can be obtained. It shows that when more than 24 internal nodes are used, the relative error is always very small.

The influence of the different parameter r_j has also been studied. The relative errors of the first and second eigenvalue are shown in Figs. 4 and 5. The relative error of the first eigenvalue is less than 0.4%, and the relative error of the second eigenvalue is less than 0.2%. It can be seen that the influence of the parameter is not significant. When $r_j \ge 0.5$ h and $1.8 \ge r_j/c_j \ge 0.1$, the computation error is rather small.

6.2. Irregular quadrilateral cavity with Neumann boundary condition

To demonstrate the capability of the present method for the irregular acoustic cavity, we next consider an irregular quadrilateral cavity as shown in Fig. 6. This example has no exact solution. A total 42 nodes are arranged on the boundary and 32 internal nodes are used for RBF interpolation. The first five eigenfrequencies are given in Table 2, the results of the other method from Ref. [36] are also shown for comparison (N_{el} represents the number of elements discretized in ANSYS, N_i represents the number of internal nodes in present method). In FEM analysis, there are 1600 elements used by ANSYS, It can be seen that the present method gives very good results for the calculation of irregular cavity. Although the node number is much less than that for ANSYS analysis, the agreement of the two methods is still excellent.

According to the first five eigenfrequencies, the corresponding mode shapes have been calculated and shown in Fig. 7.

6.3. Three-dimensional rectangular parallelepiped cavity with mixed boundary condition

In order to check the effectiveness of the present method for 3D cavity with mixed boundary condition, we final consider a rectangular parallelepiped shown in Fig. 8. The dimensions, boundary conditions are shown in the figure. The exact solution for this problem is given by

$$k = \pi \sqrt{\left(\frac{m}{L_x}\right)^2 + \left(\frac{n}{L_y}\right)^2 + \left(\frac{t+1/2}{L_z}\right)^2} \quad (m,n,t = 0,1,2,\ldots) \tag{75}$$

In the present calculation, the boundary of the rectangular parallelepiped cavity is divided into six smooth surfaces. The regular distribution of 188 boundary nodes (40 nodes on surface ABCE and EFGH each, 30 nodes on surface ABHE and DCGF each, 24 nodes on surface ADFE and BCGH each) and 120 internal nodes are used.

The first four eigenvalues are listed in Table 3. In order to test the efficacy of the method, the results of the DRHBNM and the exact solution are shown for comparison, the solutions by multiple reciprocity method (MRM) [4] with 24 elements and 94 elements are also shown in it. It can be observed that the

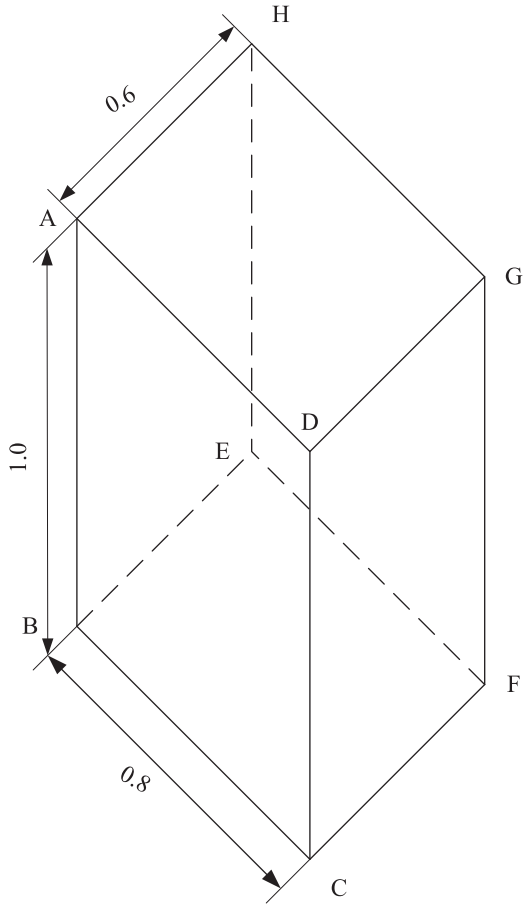

Fig. 8. Rectangular parallelepiped cavity.

Table 3
First four lowest eigenvalues of the rectangular parallelepiped cavity.

Modes (m,n,t)	Exact solution	Present method	Error (%)	MRM 24 elements	Error (%)	MRM 94 elements	Error (%)
(0,0,0)	1.571	1.582	0.7	1.64	4.5	1.59	1.3
(0,1,0)	4.230	4.237	0.2	4.44	5.0	4.28	1.2
(0,0,1)	4.712	4.725	0.3	4.76	1.1	4.71	0.0
(1,0,0)	5.466	5.498	0.6	5.60	2.4	5.58	2.0

present method can be used to calculate the acoustic eigenvalue problem of the 3-D cavity, and the results are accurate and efficient from the comparison with the exact solution.

7. Conclusions

A boundary-type meshless method, DRHBNM, has been applied for the acoustic eigenvalue problems. It combines HBNM and DRM, where HBNM is used to obtain the complementary solution without inhomogeneous terms and DRM is employed to deal with the inhomogeneous terms and obtain the particular solution. No elements are needed either for the interpolation or integration, only discrete nodes are constructed on the boundary of a domain, several nodes in the domain are only used to interpolate particular solution by the RBF.

The use of several internal nodes is important in most cases especially for higher eigenfrequencies modes, the number of the internal nodes is studied through the numerical examples. It is observed that the number of internal nodes $L=N/2$, where N is the number of boundary nodes, provides solutions which are satisfactory for acoustic eigenvalue problems.

Based on the numerical examples, the size of the sub-domain radius is also been studied. The final optimal value of the radius is between 0.8 and 0.9 h. The influence of the parameter r_j/c_j is insignificant and can be chosen from 0.1 to 1.8.

The numerical examples of regular and irregular acoustic cavity with different boundary conditions have been given and the numerical results have demonstrated the accuracy, convergence and effectiveness of the present method. The present method is a truly meshless method and can reduce greatly the pre-processing work. It is convenient to apply to the complex and practical problems.

Acknowledgements

This research work was supported by Natural Science Foundation of China (No. 50808090) and Specialized Research Fund for the Doctoral Program of Higher Education of China (No. 20070487403).

References

[1] Harris CW, Feshbach H. On the acoustic of coupled rooms. J Acoust Soc Am 1950;22:572–8.
[2] Zhao S. On the spurious solutions in the high-order finite difference methods for eigenvalue problems. Comput Methods Appl Mech 2007;196:5031–46.
[3] Petyt M, Koopman GH, Pinnington RJ. Acoustic modes of rectangular cavity with a rigid incomplete partition. J Sound Vib 1997;53:71–82.
[4] Ali A, Rajakumar C, Yunus SM. Advances in acoustic eigenvalue analysis using boundary element method. Comput Struct 1995;56:837–47.
[5] Kamiya N, Ando E, Nogae K. A new complex-valued formulation and eigenvalue analysis of the Helmholtz equation by boundary Element Method. Adv Eng Software 1996;26:219–27.
[6] Chen JT, Huang CX, Chen KH. Determination of spurious eigenvalues and multiplicities of true eigenvalues using the real-part dual BEM. Comput Mech 1999;24(1):41–51.
[7] Yeih W, Chen JT, Chen KH, Wong FC. A study on the multiple reciprocity method and complex-valued formulation for the Helmholtz equation. Adv Eng Software 1998;29(1):7–12.
[8] Chen JT. Recent development of dual BEM in acoustic problems. Comput Methods Appl Mech 2000;188:1–15.
[9] Karageorghis A. The method of fundamental solutions for the calculation of the eigenvalues of the Helmholtz equation. Appl Math Lett 2001;14:837–42.
[10] Chen JT, Chang MH, Chen KH, Chen IL. Boundary collocation method for acoustic eigenanalysis of three-dimensional cavities using radial basis function. Comput Mech 2002;29:392–408.
[11] Christina W, Otto VE. Dispersion analysis of the meshfree radial point interpolation method for the Helmholtz equation. Int J Numer Meth Eng 2009;77:1670–89.
[12] Nayroles B, Touzot G, Villon P. Generalizing the finite element method: diffuse approximation and diffuse element. Comput Mech 1992;10:307–18.
[13] Belytschko T, Lu YY, Gu L. Element-free Galerkin methods. Int J Numer Meth Eng 1994;137:229–56.
[14] Liu WK, Chen Y, Uras RA, Chang CT. Generalized multiple scale reproducing kernel particle methods. Comput Methods Appl Mech Eng 1996;139:91–157.
[15] Liu GR, Gu YT. A local point interpolation method for stress analysis of two-dimensional solids. Struct Eng Mech 2001;11:221–36.
[16] Atluri SN, Zhu T. A new meshless local Petrov–Galerkin approach in computational mechanics. Comput Mech 1998;22:117–27.
[17] Gu YT, Liu GR. A coupled elementfree Galerkin/boundary element method for stress analysis of two-dimensional solids. Comput Methods Appl Mech 2001;190:4405–19.
[18] Liu GR. In: Mesh-free methods: moving beyond the finite element method. Boca Raton, London, New York, Washington: CRC Press; 2003.
[19] Mukherjee YX, Mukherjee S. The boundary node method for potential problems. Int J Numer Meth Eng 1994;140:797–815.
[20] Chen W, Tanaka M. A meshless, exponential convergence, integration-free, and boundary-only RBF technique. Comput Math Appl 2002;43:379–91.
[21] Jin BT, Chen W. Boundary knot method based on geodesic distance for anisotropic problems. J Comput Phys 2006;215(2):614–29.
[22] Zhang JM, Yao ZH, Li H. A hybrid boundary node method. Int J Numer Meth Eng 2002;53:51–63.
[23] Zhang JM, Yao ZH, Masataka Tanaka. The meshless regular hybrid boundary node method for 2-D linear elasticity. Eng Anal Bound Elem 2003; 127:259–68.
[24] Zhang JM, Yao ZH. The regular hybrid boundary node method for three-dimensional linear elasticity. Eng Anal Bound Elem 2004;28:525–34.
[25] Zhang JM, Tanaka Masataka, Matsumoto Tosiro. Meshless analysis of potential problems in three dimensions with the hybrid boundary node method. Int J Numer Meth Eng 2004;59:1147–68.
[26] Miao Y, Wang YH, Yu F. Development of hybrid boundary node method in two-dimensional elasticity. Eng Anal Bound Elem 2005;29:703–12.
[27] Miao Y, Wang YH. An improved hybrid boundary node method in two dimensional solids. Acta Mech Solida Sin 2005;18(4):307–15.
[28] Miao Y, Wang YH. Meshless analysis for three-dimensional elasticity with singular hybrid boundary node method. Appl Math Mech Engl 2006;27(5):673–81.
[29] Miao Y, Wang Y, Wang YH. A meshless hybrid boundary node method for Helmholtz problems. Eng Anal Bound Elem 2009;33(2):120–7.
[30] SiMa YZ, Zhu HP, Miao Y. Dual reciprocity singular hybrid boundary node method for solving inhomogeneous equations. J Mech 2009;25(2):117–22.
[31] Nardini D, Brebbia CA. A new approach to free vibration analysis using boundary elements. Boundary element methods in engineering. Southampton, Berlin and New York: Computational Mechanics Publications, Springer; 1983.
[32] Wrobel LC, Brebbia CA. The dual reciprocity boundary element formulation for non-linear diffusion problems. Comput Meth Appl Mech 1987;65:147–64.
[33] Liao B, Miao Y, Luo Z. Dual hybrid boundary node method for transient eddy current problem. Appl Math Sci 2009;3(32):1567–77.
[34] Yan F, Wang YH, Miao Y, Cheung YK. Dual reciprocity hybrid boundary node method for free vibration analysis. J Sound Vib 2009;321:1036–57.
[35] Mukherjee YX, Mukherjee S. On boundary conditions in the element-free-Galerkin method. Comput Mech 1997;19:264–70.
[36] Kim YY, Kim DK. Applications of waveguide-type base functions for the eigenproblems of two-dimensional cavities. J Acoust Soc Am 1999;106(4):1704–11.